

Trends in the solubility of iron, aluminium, manganese and phosphorus in aerosol collected over the Atlantic Ocean

A.R. Baker^{a,*}, T.D. Jickells^a, M. Witt^{a,1}, K.L. Linge^b

^a *Laboratory for Global Marine and Atmospheric Chemistry, School of Environmental Sciences, University of East Anglia, Norwich, NR4 7TJ, UK*

^b *NERC ICP Facility, School of Earth Sciences and Geography, Kingston University, Kingston-upon-Thames, KT1 2EE, UK*

Received 9 December 2004; received in revised form 20 May 2005; accepted 27 June 2005

Available online 23 September 2005

Abstract

The solubility of iron, aluminium, manganese and phosphorus has been determined in aerosol samples collected between 49°N and 52°S during three cruises conducted in the Atlantic Ocean as part of the European Union funded IRONAGES programme. Solubilities (defined at pH 4.7) determined for Fe and Al in samples of Saharan dust were significantly lower (medians 1.7% and 3.0%, respectively) than the solubilities of these metals in aerosols from other source regions (whole dataset medians 5.2% and 9.0%, respectively). Mn solubility also varied with aerosol source, but the median solubility of Mn in Saharan dust was very similar to the median for the dataset as a whole (55% and 56%, respectively). The observed solubility of aerosol P was ~32%, with P solubility in Saharan aerosol perhaps as low as 10%. Laboratory studies have indicated that aerosol Fe solubility is enhanced by acid processing. No relationship could be found between Fe solubility and the concentrations of acid species (non-seasalt SO_4^{2-} , NO_3^-) nor the net acidity of the aerosol, so we are unable to confirm that this process is significant in the atmosphere. In terms of the supply of soluble Fe to oceanic ecosystems on a global scale, the observed higher solubility for Fe in non-Saharan aerosols is probably not significant because the Sahara is easily the dominant source of Fe to the Atlantic. On a smaller scale however, higher solubility for aerosol Fe may alter our understanding of Fe cycling in regions such as the remote Southern Ocean.

© 2005 Elsevier B.V. All rights reserved.

Keywords: Aerosols; Solubility; Iron; Phosphorus; Atlantic Ocean

1. Introduction

The deposition of atmospheric aerosols to the surface ocean is believed to play a significant role in supplying trace metals, including the important micro-nutrient Fe, and the major nutrients N and P to the

remote ocean. While the majority of N-containing species in aerosol are readily soluble (Paerl, 1997; Baker et al., 2003), both Fe and P are present in aerosol in forms that are only slightly soluble in seawater (Graham and Duce, 1982; Jickells and Spokes, 2001). Thus determination of the impact of atmospheric Fe and P inputs to the ocean requires knowledge of the solubility of these elements in addition to their total deposition.

The solubility of aerosol Fe is a key uncertainty in our understanding of the marine cycle of Fe and, through the links between Fe concentration and phytoplankton growth, the global carbon cycle. A number of studies, working primarily on desert dust or soil and/or

* Corresponding author. Tel.: +44 1603 591529; fax: +44 1603 591327.

E-mail address: alex.baker@uea.ac.uk (A.R. Baker).

¹ Current address: Department of Chemistry and Biochemistry, University of North Carolina at Wilmington, 601 S. College Road, Wilmington, NC 28403, United States.

urban aerosol, have reported aerosol Fe solubility estimates (see the synthesis in Jickells and Spokes, 2001 and later works Bonnet and Guieu, 2004; Hand et al., 2004). There is a considerable range (0.001–80%) in these solubility estimates and a number of factors, such as suspended particle concentration (Zhuang et al., 1992; Spokes and Jickells, 1996; Bonnet and Guieu, 2004), chemical–photochemical atmospheric processing of aerosol particle surfaces (Spokes et al., 1994; Hand et al., 2004) and aerosol source (Spokes et al., 1994), have been suggested to influence aerosol Fe solubility. A contributing factor to the wide range of Fe solubility estimates is the similarly diverse range of techniques used in the above studies. There is still much debate as to what is the ‘true’ solubility of aerosol Fe and how this solubility is related to the fraction of deposited Fe that is available for phytoplankton growth (Jickells et al., 2005; Mahowald et al., in press-b).

In addition to dissolution of Fe from mineral aerosols, a number of other biogeochemically important elements (including Al, Mn and P) are also supplied to the water column by dust deposition. Measures et al. (Measures and Brown, 1996; Measures and Vink, 2000) have used dissolved Al concentrations in surface seawater to estimate mineral dust inputs to the ocean. Understanding of the solubility of aerosol Al is central to this approach (Measures and Vink, 2000). Dissolved Al concentrations are affected by biological activity to a lesser extent than dissolved Fe concentrations, so that comparison to dissolved Fe may provide information on biological Fe removal. The residence times of dissolved Fe, Al and Mn in surface seawater are also rather different (Orians and Bruland, 1985; Jickells, 1999; Sarthou et al., 2003), so that determination of their concentrations in the water column offers the possibility to examine dust inputs over very different time-scales.

Atmospheric inputs of P to the ocean appear to be small relative to the other main nutrients N and Fe (Baker et al., 2003), but may be important since phytoplankton growth in some areas of the ocean may be (co-)limited by P (Mills et al., 2004). There is very little data on the solubility of aerosol P, but Graham and Duce (1982) estimated its solubility in aerosol collected over the northwestern Atlantic to be around 36%, and similar values have been reported for aerosol samples collected at coastal sites in Israel (Herut et al., 1999). Ridame and Guieu (2002) reported that up to 15% of P in the <20 μm fraction of an Algerian soil, considered a proxy for Saharan aerosol, was soluble in seawater.

Here we present solubility estimates for Fe, Al and Mn in aerosol samples collected during three cruises in the Atlantic Ocean conducted under the European

Union-funded IRONAGES programme. By sampling over a wide latitude range (Fig. 1), we have collected aerosol influenced by urban/industrial emissions, desert dust inputs and biomass burning, as well as aerosol from the remote North and South Atlantic. Thus our solubility estimates consider real aerosol samples rather than end-member source materials. Metal solubility values are based on a soluble metal leach of the aerosols at pH 4.7. For one of the cruises P solubility estimates (based on a soluble leach at pH 7) are also presented. Our methods do not allow us to reproduce aerosol component solubility in seawater directly, but the trends in solubility we observe should be reflected in the environmental behaviour of the aerosol on deposition to seawater. We discuss our results in terms of the

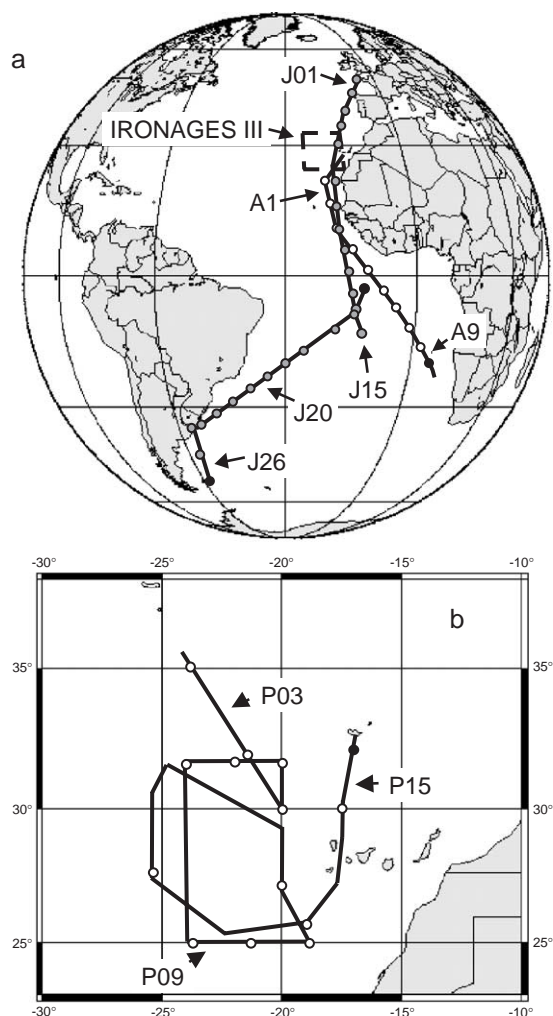


Fig. 1. Aerosol sampling start locations and cruise tracks. (a) ANT18-1 (white), JCR (grey) and IRONAGES III study area; (b) IRONAGES III. Selected sample numbers are indicated. Black markers indicate end of sampling.

influence of aerosol source, concentration and chemical processing, and focus our discussion primarily on Fe because of its importance as a key limiting nutrient in the oceans.

2. Methods

Aerosol samples were collected during three cruises in the Atlantic Ocean (Fig. 1). Cruise ANT18-1 sailed from Bremerhaven, Germany to Cape Town, South Africa (29th September–23rd October 2000, Table 1) aboard RV *Polarstern* (Sarthou et al., 2003). The second cruise was aboard RRS *James Clark Ross* (JCR) from Grimsby, UK to Port Stanley, Falkland Islands (10th September–24th October 2001) (Baker et al., 2003), during which sampling was interrupted briefly twice, once by other work in the vicinity of Ascension Island and once by a port call at Montevideo (Table 2). The third cruise, IRONAGES III (RV *Pelagia*, Azores-Valencia, 3rd–29th October 2002, Table 3), operated in the area of the Canary Basin (Kramer et al., 2004). Wind direction was continually monitored during sample collection and the samplers were turned off if there was a risk of sample contamination from the ships' stack smoke.

Two high volume ($1 \text{ m}^3 \text{ min}^{-1}$) aerosol collectors were used on all cruises to collect paired samples for trace metal (TM) and major ion (MI) analysis. In some cases (TM for ANT18-1 and JCR, MI also for JCR) the collectors were equipped with cascade impactors for size segregation of the aerosol, otherwise bulk (unsegregated) aerosol sampling was employed. For size-segregated samples, we report our results in terms of a size split of $1 \mu\text{m}$ (impactor stages 3 and 4 $> 1 \mu\text{m}$, backup filter $< 1 \mu\text{m}$) as this represents the boundary between the fine particles that are generated in the atmosphere by gas-to-particle conversions and the coarse material

Table 2

Details of trace metal aerosol sample collection for JCR cruise^a

Sample number	Start date	Start position	End date	End position	Air volume (m^3)
J01	12/9/01	48.6N 6.3W	13/9/01	44.5N 9.5W	1352
J02	13/9/01	44.3N 9.7W	14/9/01	39.8N 12.9W	1356
J03	14/9/01	39.1N 13.4W	15/9/01	35.1N 15.2W	1182
J04	15/9/01	34.9N 15.3W	16/9/01	30.3N 17.0W	1425
J05	16/9/01	30.2N 17.0W	17/9/01	26.0N 18.0W	1147
J06	17/9/01	26.0N 18.0W	18/9/01	21.2N 18.5W	1293 ^b
J07	18/9/01	21.1N 18.5W	19/9/01	15.7N 18.5W	1578
J08	19/9/01	15.5N 18.5W	20/9/01	10.7N 18.2W	1412
J09 ^c	20/9/01	10.4N 18.2W	21/9/01	6.0N 17.3W	1388
J10	21/9/01	5.8N 17.2W	22/9/01	1.3N 16.3W	1420
J11	22/9/01	1.1N 16.3W	23/9/01	3.5S 15.3W	1461
J12	23/9/01	3.8S 15.3W	24/9/01	7.8S 14.4W	1278
J13	24/9/01	7.6S 14.3W	25/9/01	2.6S 12.6W	1586
J14	30/9/01	7.9S 13.4W	1/10/01	10.6S 13.1W	0 ^d
J15	5/10/01	12.6S 14.6W	6/10/01	9.2S 13.3W	1161
J16	7/10/01	8.3S 15.0W	8/10/01	11.3S 19.1W	1404 ^b
J17	8/10/01	11.4S 19.2W	10/10/01	16.3S 26.0W	2363
J18	10/10/01	16.4S 26.2W	11/10/01	19.1S 30.0W	1402
J19	11/10/01	19.2S 30.1W	12/10/01	22.1S 34.4W	1449
J20	12/10/01	22.2S 34.5W	13/10/01	25.1S 38.7W	1368
J21	13/10/01	25.1S 38.7W	13/10/01	26.3S 40.6W	687
J22	14/10/01	28.1S 43.3W	15/10/01	31.1S 47.9W	1491
J23	15/10/01	31.2S 48.1W	16/10/01	34.1S 52.7W	1444
J24	16/10/01	34.2S 52.9W	16/10/01	34.8S 53.8W	324
J25	19/10/01	35.0S 56.0W	21/10/01	42.5S 56.4W	2550
J26	21/10/01	42.7S 56.5W	23/10/01	51.6S 57.6S	2729

^a Major ion samples were collected in parallel with TM samples, details for TM samples only are shown.

^b Two samples collected as a day/night pair, reported here as a single sample for consistency.

^c TM sample was contaminated with rain water during passage through the Inter-tropical Convergence Zone. Sample not analysed.

^d Exposure blank. Filters were deployed in collectors but motors were not switched on.

whose source is mechanical (e.g. soil-derived dust, seaspray particles) (Raes et al., 2000). For the JCR

Table 1

Details of trace metal aerosol sample collection for ANT18-1 cruise^a

Sample number	Start date	Start position	End date	End position	Air volume (m^3)
	8/10/00		9/10/00		0 ^b
	9/10/00		10/10/00		0 ^c
A1	10/10/00	21.1°N 20.7°W	11/10/00	16.1°N 19.8°W	1317.9
A2	11/10/00	15.9°N 19.7°W	12/10/00	10.6°N 18.6°W	1487.2
A3	12/10/00	10.4°N 18.6°W	13/10/00	6.0°N 15.3°W	1487.4
A4	13/10/00	5.7°N 15.1°W	14/10/00	1.6°N 11.7°W	1359.9
A5	14/10/00	1.4°N 11.6°W	15/10/00	2.8°S 8.2°W	1441.7
A6	15/10/00	3.1°S 8.0°W	16/10/00	6.7°S 5.1°W	1173.0
A7	16/10/00	6.9°S 4.9°W	17/10/00	11.4°S 1.3°W	1470.9
A8	17/10/00	11.5°S 1.2°W	18/10/00	15.6°S 2.2°E	1416.3
A9	18/10/00	15.8°S 2.3°E	19/10/00	19.6°S 5.5°E	1364.2

^a Major ion samples were collected in parallel with TM samples, details for TM samples only are shown.

^b Operational blank. Filter mounted in cassette, but not deployed in collector.

^c Exposure blank. Filters were deployed in collectors but motors were not switched on.

Table 3
Details of trace metal aerosol sample collection for IRONAGES III cruise^a

Sample number	Start date	Start position	End date	End position	Air volume (m ³)
P01					0 ^b
P02					0 ^c
P03	5/10/02	35.1N 23.8W	6/10/02	32.0N 21.5W	1725
P04	6/10/02	32.0N 21.5W	7/10/02	30.0N 20.0W	1699
P05	7/10/02	30.0N 20.0W	8/10/02	31.7N 20.0W	1652
P06	8/10/02	31.7N 20.0W	9/10/02	31.7N 22.0W	577
P07	9/10/02	31.7N 22.0W	10/10/02	31.6N 24.0W	1373
P08	10/10/02	31.6N 24.0W	13/10/02	25.0N 23.8W	2488
P09	13/10/02	25.0N 23.8W	14/10/02	25.0N 21.3W	1479
P10	14/10/02	25.0N 21.3W	15/10/02	25.0N 18.9W	1808
P11	15/10/02	25.0N 18.9W	16/10/02	27.2N 20.0W	2100
P13	20/10/02	27.4N 25.4W	22/10/02	25.7N 19.0W	3642
P14	22/10/02	25.7N 19.0W	24/10/02	30.0N 17.5W	1096
P15	24/10/02	30.0N 17.5W	25/10/02	32.1N 17.0W	680

^a Major ion samples were collected in parallel with TM samples, details for TM samples only are shown.

^b Operational blank. Filter mounted in cassette, but not deployed in collector.

^c Exposure blank. Filters were deployed in collectors but motors were not switched on.

cruise we also report results for bulk aerosol, i.e. the sum of the fine and coarse modes. Aerosol collection substrates (slotted and backup filters) were all Whatman 41 paper. (Coarse TM aerosol was collected on quartz fibre substrates during ANT18-1 (Sarthou et al., 2003). These gave acceptable results for soluble metal analysis (after washing) but the blanks associated with total metal analysis were too high to allow reliable solubility estimates to be determined. Results for metal solubility for fine mode aerosols only are reported for ANT18-1 here). Substrates used for TM sampling were acid-washed before use (see Table 4 for details), rinsed with copious amounts of ultrapure water after each

soak, and were dried overnight under a laminar flow clean bench before being sealed in zip-lock plastic bags ready for use. Substrates for MI sampling were used without any pre-treatment. Aerosol collection substrates were handled aboard ship under a laminar flow clean bench, and exposed substrates were transferred to individual zip-lock plastic bags immediately after collection and stored frozen until analysis at UEA. Laboratory sample manipulation was carried out under uniform light conditions in a laminar flow clean bench housed in a trace metal-clean laboratory.

Total and soluble metals (and total and soluble phosphorus for JCR) were all extracted from fractions of the TM aerosol samples. The aerosol filter fractions used (Table 5) were determined by weighing portions of the (previously weighed) exposed filters, which had been cut into small pieces using acid-cleaned ceramic-bladed scissors. Soluble metals were extracted using an ammonium acetate leach at pH 4.7 for 1–2 h (Sarthou et al., 2003). This pH was chosen initially as a mimic for release of trace metals from aerosol in rainwater, but is similar to a procedure employed by Bruland et al. (2001) to examine the bioavailable Fe content of upwelled particulate matter off the coast of California. The implications of this choice in terms of ‘true’ solubility in seawater are discussed below (Section 3.6). Metal (Fe, Al, Mn) concentrations in extracts were determined by graphite furnace atomic absorption spectroscopy (GFAAS), or by inductively coupled plasma-optical emission spectroscopy (ICP-OES) for IRONAGES III. Extraction of soluble phosphorus was achieved using ultrasonic agitation for 1 h in a 1 mM NaHCO₃ solution to buffer the extract at pH 7 (Baker et al., 2003), as the lower pH of the ammonium acetate buffer interferes with the analysis of soluble P. Preliminary trials indicated that the fraction of total P released as ‘soluble’ was pH depen-

Table 4
Cleaning protocols used for TM aerosol sampling substrates for ANT18-1, JCR and IRONAGES III cruises, associated filter blank values and atmospheric detection limits^a

Cruise	Filter washing solutions	Total metal blanks	Total metal detection	Soluble metal	Soluble metal detection
		(nmol/filter)	limits (pmol m ⁻³)	blanks (nmol/filter)	limits (pmol m ⁻³)
		Fe, Al, Mn, P ^b	Fe, Al, Mn, P ^b	Fe, Al, Mn, P ^b	Fe, Al, Mn, P ^b
ANT18-1	2 L 0.1 M HCl	b-155, 523, 3.8	b-31, 56, 1.9	b-29, 22, 0.7 s-35, 76, 1.0	b-13, 8, 0.3 s-9, 40, 0.5
JCR	4 L 0.1 M HCl, 2 L 1 M NH ₄ OAc	b-276, 137, 5.3, 114 s-51, 204, 1.9, 86	b-69, 24, 0.9, 18 s-28, 126, 1.1, 24	b-9.2, 6.9, 0.3, 0.1 s-1.1, 2.8, 0.5, 3.0	b-0.6, 7.1, 0.1, 3.2 s-0.6, 9.9, 1.3, 0.7
IRONAGES III	2 L 10% HCl, 2 L 1% HNO ₃	101, 44, 3.1	24, 39, 0.02	2.1, 2.8, 0.2	0.9, 0.1, 0.1

s denotes slotted, upper stages of cascade impactor (coarse mode); b denotes backup filter (fine mode).

^a Calculated using 3σ of the blank and an air volume of 1400 m³.

^b JCR cruise only.

Table 5
Summary of extraction conditions used for analytes determined in TM and MI aerosol samples for ANT18-1, JCR and IRONAGES III cruises

Analyte	Filter type	Filter fraction ^a	Extract
<i>ANT18-1</i>			
Soluble Fe, Al, Mn	TM	0.10 (s), 0.25 (b)	25 mL 1.1 M NH ₄ OAc (pH 4.7)
Total Fe, Al, Mn	TM	0.015 (s), 0.02 (b)	5 mL conc HNO ₃ /1 mL conc HF
<i>JCR</i>			
Soluble Fe, Al, Mn	TM	0.10 (s), 0.25 (b)	25 mL 1.1 M NH ₄ OAc (pH 4.7)
Soluble P	TM	0.25 (s), 0.2 (b)	9 mL 1 mM NaHCO ₃ (pH 7)
Total Fe, Al, Mn, P	TM	0.05 (s), 0.11 (b)	6 mL conc HNO ₃ /1 mL conc HF
Major ions	MI	0.25 (s, b)	25 mL ultrapure water
<i>IRONAGES III</i>			
Soluble Fe, Al, Mn	TM	0.25 ^b	25 mL 1.1 M NH ₄ OAc (pH 4.7)
Total Fe, Al, Mn	TM	0.03125	6 mL conc HNO ₃ /1 mL conc HF

s denotes slotted, upper stages of cascade impactor (coarse mode); b denotes backup filter (fine mode).

^a Fraction of substrate used for each analysis.

^b Results presented in Fig. 9 were obtained using filter fractions of 0.25, 0.125, 0.063 and 0.031.

dent, increasing with decreasing pH. Hence extraction in unbuffered solution (as for major ions, below) was not practical, since extract pH may vary significantly in unbuffered samples due to changing relative contributions from acidic (e.g. SO₄²⁻, NO₃⁻) and alkaline (e.g. NH₄⁺, HCO₃⁻, CO₃²⁻) species. Extracted phosphorus was determined spectrophotometrically as soluble reactive phosphorus using the method of Parsons et al. (1984). A strong acid digestion procedure was used to determine total Fe, Al, Mn and P. Filter portions were boiled to dryness firstly in 69% HNO₃ and then in 40% HF to destroy organic matter (including the cellulose filter) and the aluminosilicate matrix of the mineral component of the aerosol. The residue was redissolved in 1 M HNO₃, transferred quantitatively to volumetric flasks (25 or 50 mL) and made up to volume. Analysis for total Fe, Al and Mn was by ICP-OES, or in a few cases, where concentrations were near or below the detection limit for ICP-OES, by GFAAS. Total P was analysed by high resolution magnetic sector inductively coupled plasma mass spectrometry (HR-ICP-MS). HR-ICP-MS overcomes the traditional limitations of P analysis by quadrupole ICP-MS because it is more sensitive and is able to resolve the P signal from polyatomic interferences at mass 31 that are derived from N, O and H in the sample matrix. The final acidity of the samples was typically about 3% HNO₃, which lead to increased formation of ¹⁴N¹⁶O¹H⁺, in particular. However, a resolution of 1500 was sufficient to resolve P from all interferences and a detection limit of 3 nmol P L⁻¹ was achieved.

Major ions (Na⁺, Mg²⁺, K⁺, Ca²⁺, NH₄⁺, Cl⁻, NO₃⁻, SO₄²⁻) were determined by ion chromatography after extraction of a quarter of the MI filters in ultrapure

water with one hour of ultrasonic agitation (Baker et al., 2003; Jickells et al., 2003).

For each of the analyses described above, procedural blanks were determined in every batch of analyses by carrying out identical extraction procedures in sample vessels which did not contain aerosol samples. These procedural blanks have been subtracted from the results for each batch.

Aerosol collection operational blanks were assessed by analysing filters that had been treated as for samples (acid-washed in the case of TM filters, unwashed for MI), but which were not otherwise used. During each cruise one set of filters was also mounted in the aerosol collectors for 24 h without the collector pump in operation to give an indication of the operational blank associated with the sampling procedure. This 'exposure blank' however probably over-estimates the operational blank because the filters are subject to passive deposition of aerosol particles during exposure, and this process does not occur during normal sample collection. Limits of detection for the analytes reported here (Table 4) are governed by the uncertainties in the operational (filter) blank, rather than the instrumental detection limits for each analysis.

Concentrations in extracts were converted into atmospheric concentrations by calculating the total quantity of analyte on each filter, after appropriate (procedural and operational) blank correction, and dividing by the known volume of air filtered for each sample. Uncertainties quoted for atmospheric concentrations have been calculated from standard deviations of replicate analyses and propagated for each stage of data analysis (blank subtraction, etc.) by standard error propagation methods. The percentage

solubility (Sol_x , $X = \text{Fe, Al, Mn or P}$) was calculated as:

$$\text{Sol}_x = 100 * X^{\text{sol}} / X^{\text{total}} \quad (1)$$

where X^{sol} and X^{total} are the soluble and total atmospheric concentrations of each component.

The component of major ion concentrations arising from seasalt (ssMI) was determined using Na^+ as a reference species for aerosol seaspray content, see (Baker, 2004). Aerosol non-seasalt concentrations were derived by subtracting this value from the total aerosol concentration ($\text{nssMI} = \text{MI} - \text{ssMI}$). Air mass back trajectories for arrival heights of 10, 500 and 1000 m above the ship's position were obtained from the NOAA Air Resources Laboratory (HYSPLIT model, FNL data set; Draxler and Rolph, 2003), and were used together with chemical data to indicate aerosol source.

3. Results and discussion

3.1. Air masses

Examples of 5-day air mass back trajectories encountered during the ANT18-1, JCR and IRONAGES III cruises are shown in Fig. 2. In the temperate and subtropical North Atlantic air mass arrivals were generally from the north (air mass type NATl/Rem: samples J04, J05, P06–P11, P13–P15). There was some contact of northerly air with European land masses for samples J01–J03 (NATl/Eur) and minimal contact with land in a few cases for the IRONAGES III cruise (P06–P08, northern Canada and P11 and P14, Canary Islands). Samples that contained visible, orange-brown Saharan dust (Sahara: A1–A3, J06–J08, P03–P05) were characterised by surface level air mass arrivals from the north-east and upper level (>500 m) trajectory arrivals from West Africa. The southern boundary of Saharan dust extent was marked by the Intertropical Convergence Zone (ITCZ), which was crossed during collection of samples A3 (ANT18-1; Sarthou et al., 2003) and J09 (JCR). In the north and east of the South Atlantic air mass arrivals were predominantly southeasterly in origin (SATl/SE: A4, A5, A9, J10–J12, J15), although some samples (A6–A8, J13, J16, J17) were influenced by (easterly) upper level arrivals from southern Africa (SATl/SAfr). In the central South Atlantic remote marine air was sampled (SATl/Rem: J18–J23)—these air masses had no contact with land for at least 5 days prior to collection. The air masses sampled during J24 and the initial period of J25 passed over continental South America not long before collection (SATl/SAm). The remaining JCR air masses were predominantly from the remote

South Atlantic and South Pacific (SATl/SPac), but also passed over the southern tip of South America.

3.2. Total and soluble aerosol concentrations

Total and soluble concentrations of aerosol Fe, Al, Mn (and P for JCR) along the ANT18-1, JCR and IRONAGES III cruise tracks are shown in Figs. 3–5. These elements all show maximal total concentrations associated with the Saharan dust plume (Samples A1–A3, J06–J08 and P03–P05; Figs. 3–5a,c,e,g), and for the metals the Sahara represents overwhelmingly the dominant source to the Atlantic atmosphere. Concentrations of total P over much of the south Atlantic were higher (relative to the metal concentrations there), and were similar to those in the Saharan plume. In addition to the Saharan dust samples noted above, sample J20 also had the brown coloration associated with mineral aerosol. This sample had total Fe concentrations (Fig. 4a) significantly above any other sample from the remote South Atlantic. Air mass back trajectory analysis indicated that this sample may contain dust from the Patagonian region, with a travel time before collection of ~8 days.

Studies of aerosol concentrations covering the remote Atlantic basin generally report only total metal concentrations (Völkening and Heumann, 1990; Losno et al., 1992; Rädlein and Heumann, 1992, 1995) and often focus on Saharan dust transport across the tropical North Atlantic, e.g. (Arimoto et al., 1995). The total Al concentrations associated with Saharan dust that we observed ($4\text{--}24 \text{ nmol m}^{-3}$ for JCR, $25\text{--}220 \text{ nmol m}^{-3}$ for IRONAGES III) are well within the range of Al concentrations in dust observed at Izana, Canary Islands in September and October (Arimoto et al., 1995). Losno et al. (1992) reported total concentrations for several elements, including Fe, Al, Mn and P, in aerosol collected during an Atlantic transect cruise in 1988 (ANT7-1), along a similar track to our JCR cruise. They observed similar patterns to those shown in Fig. 4, with high concentrations associated with the Saharan dust plume and very low concentrations of Fe, Al and Mn, but not P, over the South Atlantic. For comparison, the concentration ranges of the ANT7-1 and JCR cruises in the remote South Atlantic are 0.14–0.36 (Fe), 0.48–1.8 (Al), ~0.02 (Mn) and 0.03–0.13 (P) nmol m^{-3} for ANT7-1 and 0.1–1.6 (Fe), 0.2–1.6 (Al), 0.001–0.03 (Mn) and 0.004–0.18 (P) nmol m^{-3} for JCR. The relatively strong source of P to the South Atlantic atmosphere has been linked to emissions of primary biogenic particles from tropical forests (Artaxo et al., 1988; Mahowald et al., in press-a). Baker et al. (2003) recently reported that the ratio of N to soluble P in aerosol deposition to the Atlantic (median

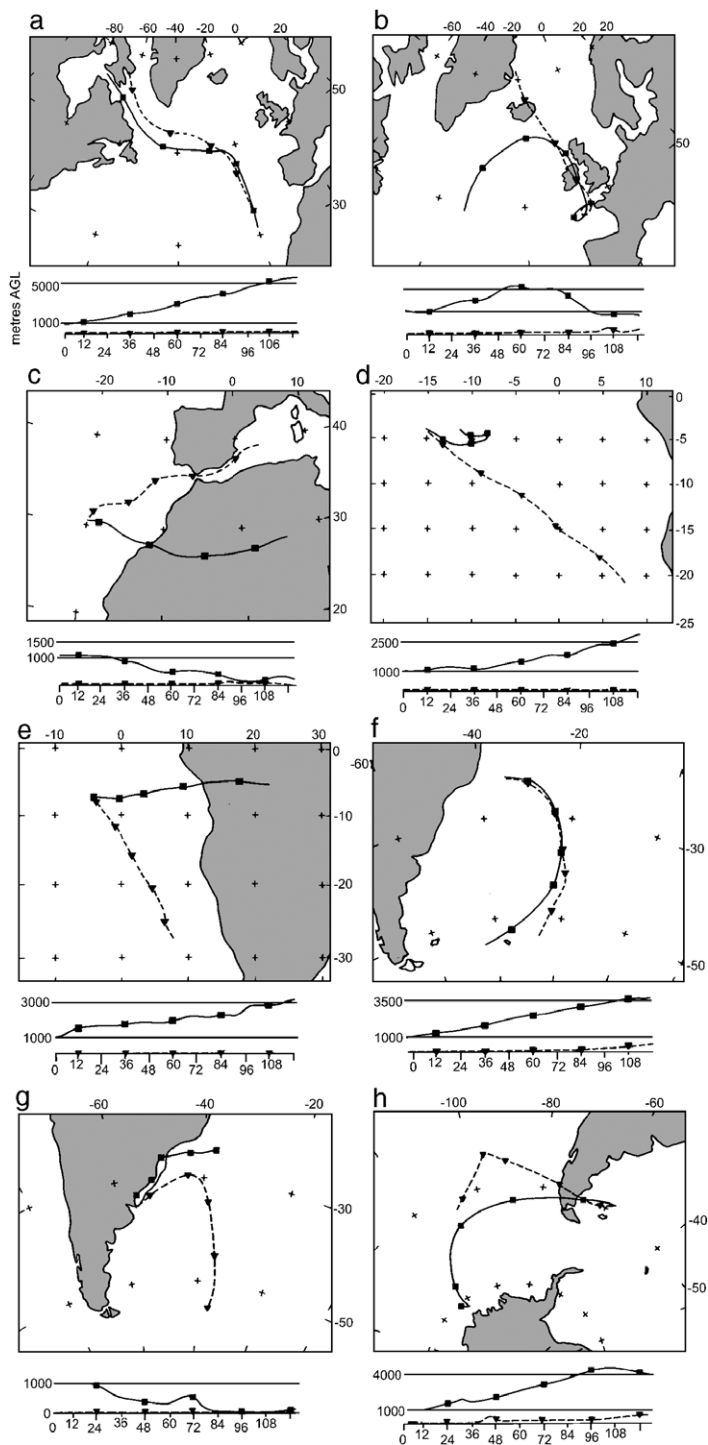


Fig. 2. Examples of 5-day air mass back trajectories for (a) NATl/Rem, (b) NATl/Eur, (c) Sahara, (d) SAtl/SE, (e) SAtl/SAfr, (f) SAtl/Rem, (g) SAtl/SAm and (h) SAtl/SPac air mass types. Air mass types are described in Section 3.1. Only arrival heights of 10 m and 1000 m above the ships' positions are shown for clarity. In the upper section of each panel the trajectories converge on the ship's position, the lower sections show variation in air mass height above ground level (AGL) with time before arrival at the ship.

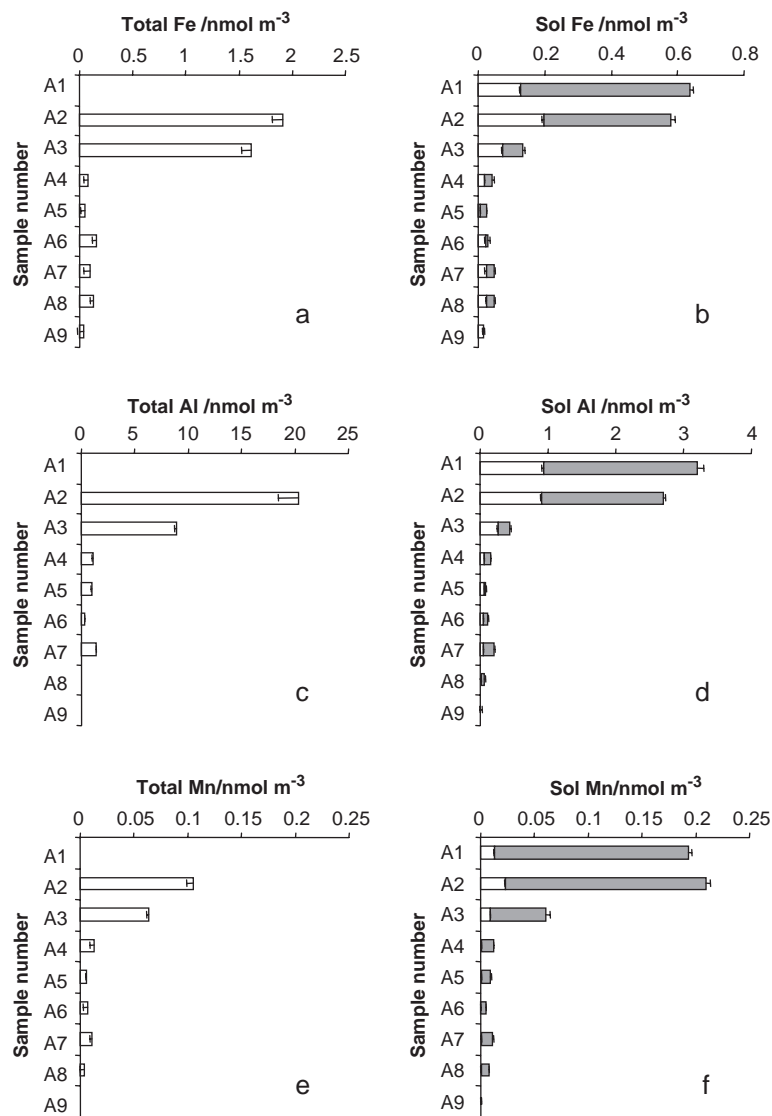


Fig. 3. Total and soluble (a and b) Fe, (c and d) Al and (e and f) Mn concentrations for the ANT18-1 cruise. White bars indicate fine mode ($<1 \mu\text{m}$) and grey bars coarse mode ($>1 \mu\text{m}$) aerosol. Only fine mode data is available for (a), (c) and (e) (see Section 2).

1200) was significantly higher than the Redfield proportion of 16:1. This implies that aerosol deposition is deficient in P in terms of phytoplankton nutrient requirements. Recalculation of the aerosol N/P using the total P data for the JCR cruise (Fig. 4g) yields values in the range 10–1400 (median 180), which confirms the P deficient status of Atlantic aerosol deposition. Losno et al. (1992) also reported that aerosol concentrations in the South Atlantic rose slightly as their cruise track neared the coast of South America and this effect may be evident also in our samples J24 and J25.

The corresponding profiles of soluble concentrations (Figs. 3–5b,d,f,h) are rather different to the total concentration profiles however. Soluble concentrations of

Fe, Al and P in non-Saharan aerosols were higher, relative to Saharan aerosols, than was the case for the total metal profiles. As discussed below, this implies that the solubility of these elements varied considerably between air mass types, with, in general, higher values for non-Saharan aerosols.

3.3. Solubility estimates

Solubility estimates were derived from the total and soluble component concentrations discussed above (Figs. 6–8). In some cases, the cumulative error in calculated solubility occasionally resulted in an uncertainty greater than 100%, usually when one or both of the total

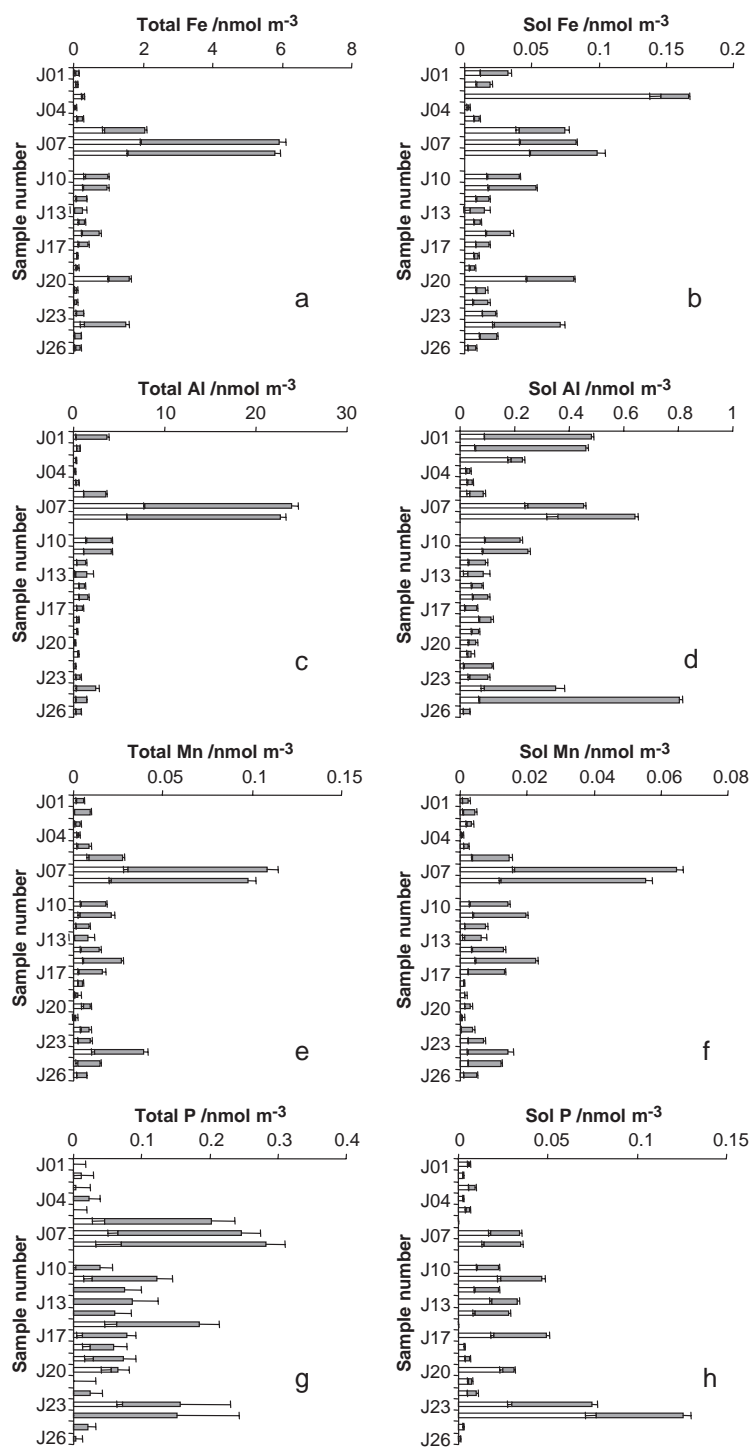


Fig. 4. Total and soluble (a and b) Fe, (c and d) Al, (e and f) Mn and (g and h) P concentrations for the JCR cruise. White bars indicate fine mode ($<1 \mu\text{m}$) and grey bars coarse mode ($>1 \mu\text{m}$) aerosol.

or soluble concentrations were very low. These data points have been excluded from our analysis and are not plotted in Figs. 6–8. This problem was particularly severe for P, where the atmospheric signal for soluble

and total P was most often close to the filter blank value. In some cases bulk P solubility values have been calculated from total concentration data in one aerosol size fraction and soluble concentration data in the other frac-

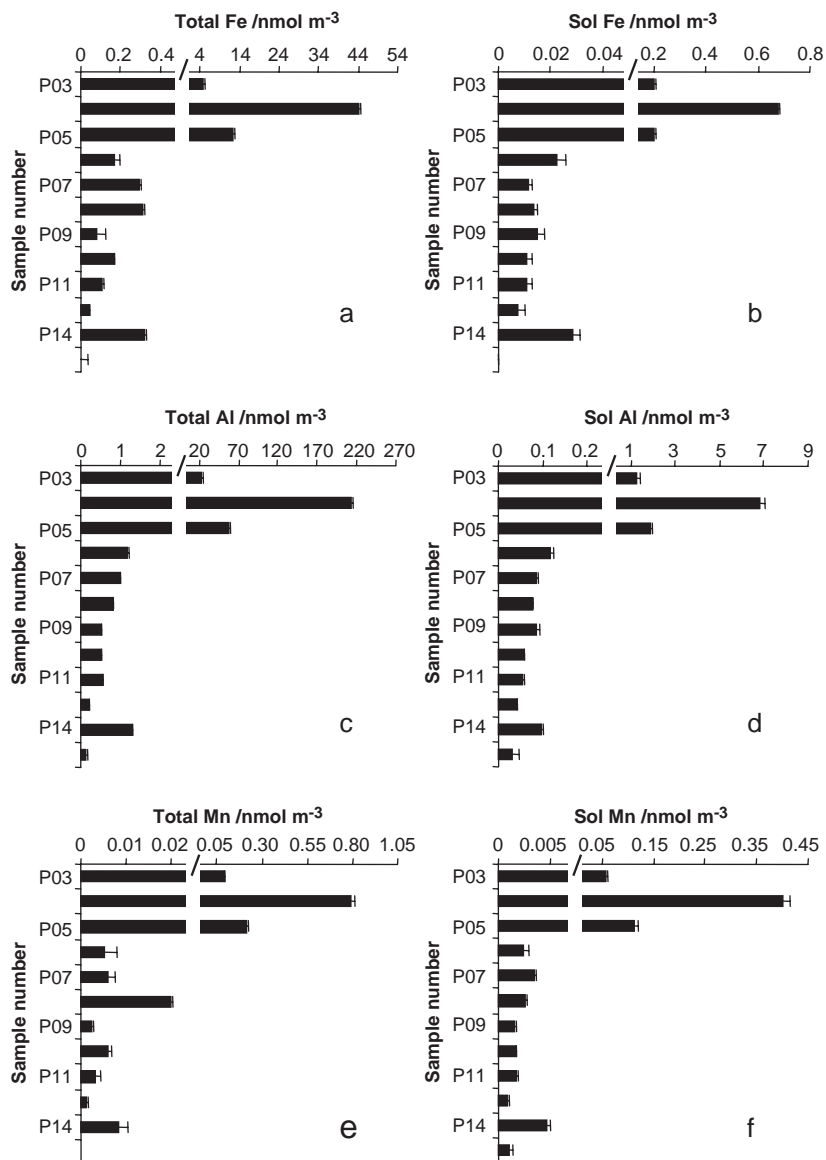


Fig. 5. Total and soluble (a and b) Fe, (c and d) Al and (e and f) Mn concentrations for the IRONAGES III cruise. Concentrations are for bulk (non-size segregated) aerosol only. Note that all x-axis scales are split.

tion only. These values (open symbols in Fig. 7h) should be treated with some caution. We include them only because of the extreme paucity of atmospheric aerosol solubility data available for P.

Ranges for solubility values in bulk aerosol (Table 6) were 1.4–54%, 1.9–86%, 13–92% and 0.01–87% for Fe, Al, Mn and P, respectively. However, for all three cruises, there were clearly systematic variations in solubility with air mass type/aerosol source.

The solubilities of Fe and Al in Saharan dust were the lowest (median 1.7% and 3.0%, respectively) of all the aerosol types sampled during our study. These

values are in good agreement with a number of other estimates for Fe and Al solubility in Saharan dust (e.g. Spokes et al., 1994; Johansen et al., 2000; Bonnet and Guieu, 2004). They are also consistent with estimates of the overall solubility of aerosol Fe (Jickells and Spokes, 2001) and Al (Gehlen et al., 2003) derived from global oceanic biogeochemical budgeting. Solubility values for Fe and Al in aerosols from non-Saharan sources were significantly higher (by factors of ~2 to >10) than for Saharan dust. The highest values were observed in aerosol of the NATl/Eur type, and this may reflect a strong anthropogenic influence on the aerosol in these

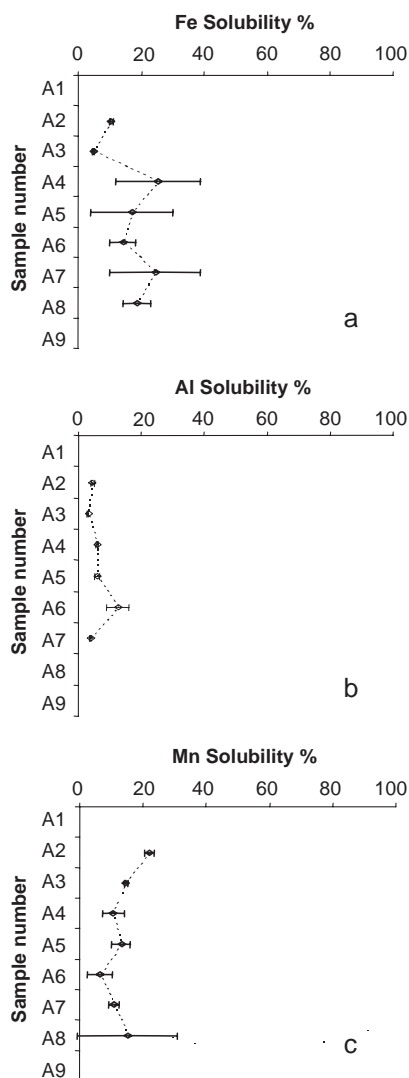


Fig. 6. Percentage solubility estimates of (a) Fe, (b) Al and (c) Mn for fine mode aerosol during ANT18-1.

samples, since urban aerosols have previously been reported to have high Fe solubility (Spokes and Jickells, 1996). However only sample J03 from this air mass type shows significant Fe enrichment over crustal abundance (Taylor and McLennan, 1985) (Enrichment Factor, $EF=5.5 \pm 1.8$), while sample J01 appears to be depleted in Fe ($EF=0.19 \pm 0.04$). In general Fe and Al solubility were higher in fine mode aerosols than coarse (Fig. 7a and c), as has been observed previously in aerosols separated at diameters of 2.5–3 μm (Siefert et al., 1999; Johansen et al., 2000; Chen and Siefert, 2004; Hand et al., 2004). However, for some samples of the NATl/Eur and SATl/Rem types coarse mode solubility was higher than fine. Trends in Fe and Al solubility in the fine and coarse mode aerosols with air mass type

were similar to those described above for the bulk aerosol, i.e. lowest values were observed for Saharan samples, with higher values for other aerosol types (Figs. 6a,b and 7a,c). Manganese solubility varied less than for Fe and Al, and its median solubility in Saharan dust was close to the median solubility of Mn in the dataset as a whole (Table 6). The amount of data available for P solubility is probably insufficient to make detailed comparison between different air mass types. However, we note that the median P solubility value for our data (32%, see Table 6) is close to the value of 36% reported for aerosol P over the north-western Atlantic (Graham and Duce, 1982), and that P solubility in Saharan dust seems to be lower than this. A similar pattern has been reported for Saharan- and European-origin aerosols (median P solubilities 25% and 45%, respectively) collected at coastal sites in Israel (Herut et al., 1999).

3.4. The particle concentration effect

A number of workers have observed that Fe solubility is a function of aerosol particle concentration, with higher solubilities observed at lower suspended particle concentration—the so-called particle concentration effect (Zhuang et al., 1992; Spokes and Jickells, 1996; Bonnet and Guieu, 2004). Because our solubility estimates are derived from soluble element determinations in which the fraction of aerosol collection substrate was held constant (Table 5), the effective total aerosol concentration in those experiments would have varied considerably between samples. For example, extractions of samples containing Saharan dust would have been carried out at much higher aerosol loadings than extractions of samples from clean south Atlantic air. This raises the possibility that our observed trends in solubility (low for Saharan samples, generally higher elsewhere) are an artefact of our experimental design. We have examined this possibility by performing soluble Fe, Al and Mn determinations on several different sized portions (Table 5) of three aerosol samples collected during the IRONAGES III cruise. Two of the samples (P04 and P05) contained Saharan dust, while the third (P08) was of north Atlantic marine origin and did not. In these experiments we have therefore obtained solubility estimates for which the total metal concentration used in the soluble metal extract varied by 2–3 orders of magnitude (Fig. 9). A striking feature of Fig. 9 is that for each metal all the solubility values obtained for the two Saharan samples are very similar to one another, regardless of the amount of sample used. In contrast, the solubility values for the non-

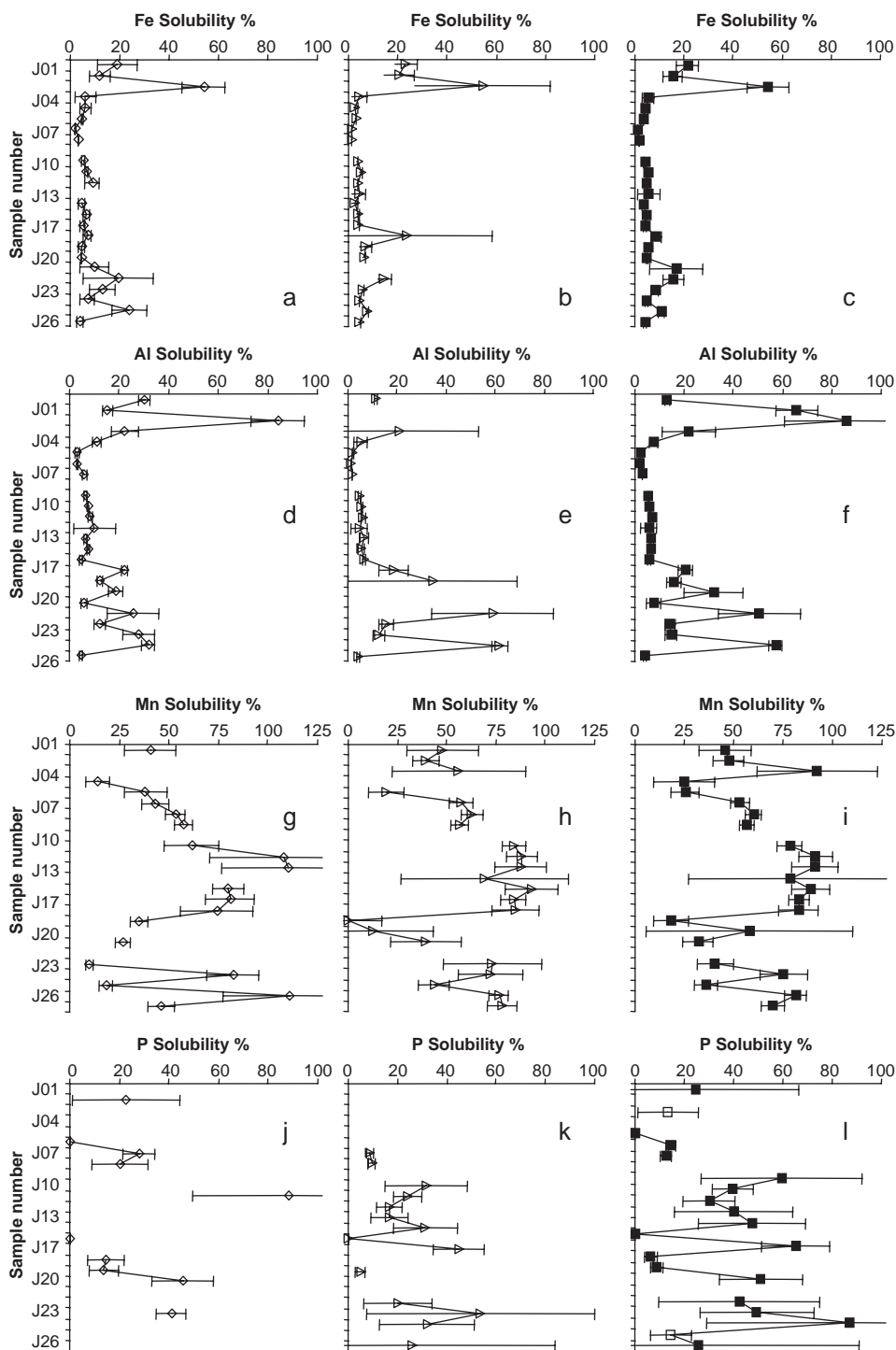


Fig. 7. Percentage solubility estimates of (a, b and c) Fe, (d, e and f) Al, (g, h and i) Mn and (j, k and l) P in fine (diamonds) and coarse (triangles) mode and bulk (solid squares) aerosol during cruise JCR.

Saharan sample are similar to one another, but significantly different from the Saharan values. Of all the metals studied, there is most evidence for the presence

of a particle concentration effect in the Mn data for the Saharan samples, but even here the effect is modest— Sol_{Mn} increases from 50 ± 2 to $58 \pm 4\%$ as the total Mn

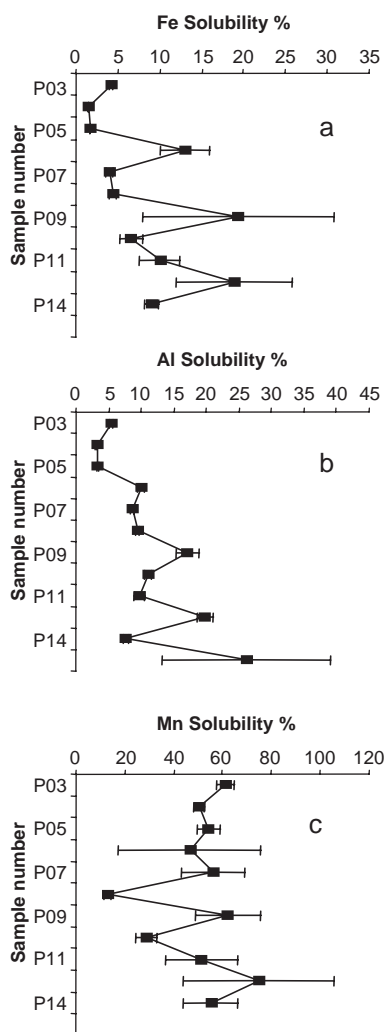


Fig. 8. Percentage solubility estimates of (a) Fe, (b) Al and (c) Mn for bulk aerosol during cruise IRONAGES III.

concentrations in the extracts decrease from 13.5 to 0.4 $\mu\text{mol L}^{-1}$. However, Sol_{Mn} for the non-Saharan sample was significantly lower (13–28%) than the Saharan

samples, so that the particle concentration effect clearly does not control Mn solubility in this case. The values of Sol_{Mn} obtained for P04/5 and P08 are very similar to those of the JCR Saharan samples J06–J08 (53–60%) and samples J04 and J05 (~25%), which had very similar air mass characteristics to P08. Therefore we believe that the particle concentration effect has a comparatively small effect on the aerosol Fe, Al, Mn (and probably also P) solubility data we report here and that the major factor controlling the observed differences in aerosol solubility is the character and origin of the aerosols themselves.

3.5. Influence of atmospheric processing on solubility

Laboratory experiments that simulate changes in aerosol pH (and ionic strength) caused by the wetting and drying cycles associated with repeated passage of aerosol particles through clouds have indicated that this atmospheric processing enhances Fe and Mn solubility (Spokes and Jickells, 1996; Desboeufs et al., 1999), though the effect is largely reversible as pH rises (Spokes and Jickells, 1996), as will happen when aerosol enters seawater. Hand et al. (2004) recently attempted to confirm whether such atmospheric chemical processing does increase solubility in the environment using data collected in regions of the remote Atlantic and Pacific Oceans influenced by desert dust inputs. They correlated Fe solubility (defined as the fraction of Fe present as Fe(II)) with non-seasalt (*nss*) SO_4^{2-} concentrations in aerosol particles with diameters $<2.5 \mu\text{m}$ and did not observe any significant relationship between these parameters. We note that the majority of *nss* SO_4^{2-} occurs in the accumulation mode ($<1 \mu\text{m}$) aerosol (Raes et al., 2000), while desert dust typically has a modal size of $\sim 2 \mu\text{m}$ (Schulz et al., 1998). Given that Hand et al. examined the $<2.5 \mu\text{m}$ aerosol fraction, it seems likely that a high proportion

Table 6

Median and range (in parentheses) percentage solubility values of Fe, Al, Mn and P in bulk aerosol sampled during JCR and IRONAGES III cruises, categorised according to the air mass types defined in the text

Air mass type	<i>n</i>	Fe	Al	Mn	P ^a
NAtl/Eur ^a	3	21, 15, 54	13, 65, 86	45, 48, 92	24
NAtl/Rem	11	7.8 (4.0–19)	10 (7.6–26)	49 (13–75)	13
Sahara	6	1.7 (1.4–4.1)	3.0 (1.9–5.5)	55 (50–64)	0.01, 14, 13
SAtl/SE ^a	4	4.5 (3.5–5.4)	6.3 (5.4–6.8)	90 (79–91)	44 (30–59)
SAtl/Afr ^a	3	5.7, 4.6, 4.4	5.6, 6.4, 6.0	79, 83, 83	40, 0.04, 65
SAtl/Rem ^a	6	8.3 (5.1–17)	18 (7.8–51)	41 (18–75)	42 (6.6–51)
SAtl/Sam ^a	2	4.7, 11	15, 57	36, 81	87, 14
SAtl/SPac ^a	1	4.2	4.2	70	26
All	36	5.2 (1.4–54)	9.0 (1.9–86)	56 (13–92)	32 (0.01–87)

Values were given for air mass type individuals with fewer than 4 available data points.

^a Data from JCR only.

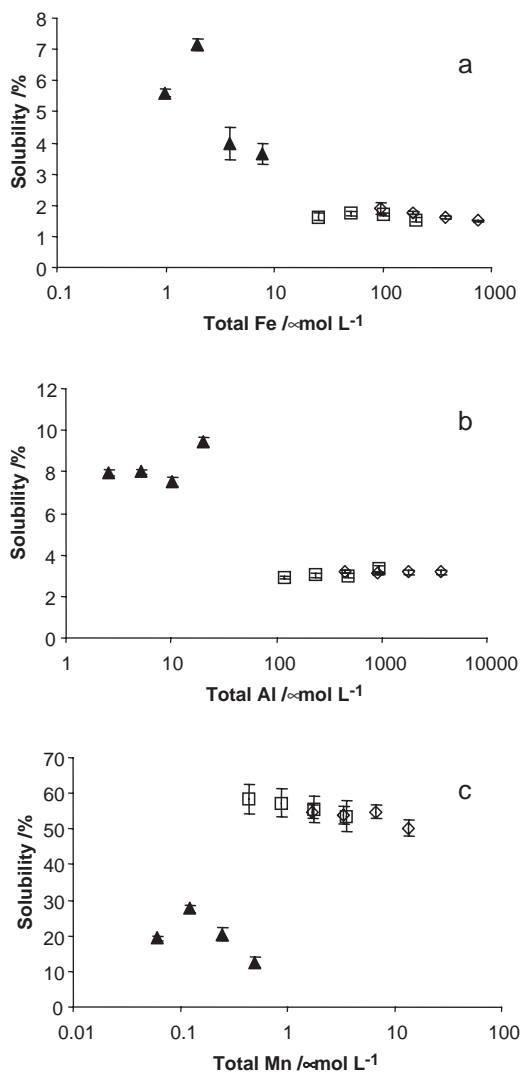


Fig. 9. The relationship between (a) Fe, (b) Al and (c) Mn solubility and their respective total concentrations in extraction solutions during experiments to determine their soluble metal fractions. Data for IRONAGES III samples P04 (open diamonds), P05 (open squares) and P08 (filled triangles) are shown.

of the nss SO_4^{2-} and Fe analysed were in separate particles that had no physical contact and, therefore a lack of correlation may be expected. In such circumstances a negative result to their test is not conclusive evidence of lack of effect and we have therefore attempted a similar analysis with our JCR data using nss SO_4^{2-} in the $<1 \mu\text{m}$ fraction and NO_3^- , the principal acid species in the $>1 \mu\text{m}$ fraction. We also find that there is no significant correlation between Fe solubility and acid species concentrations in either size fraction ($<1 \mu\text{m}$: $\text{Sol}_{\text{Fe}}/\text{nss SO}_4^{2-}$, $r^2=0.003$, $>1 \mu\text{m}$: $\text{Sol}_{\text{Fe}}/\text{NO}_3^-$, $r^2=0.10$), nor between Fe solubility and aerosol net potential acidity (i.e. the difference between total

acid species concentrations and total alkaline species concentrations; Jickells et al., 2003) ($<1 \mu\text{m}$: $\text{Sol}_{\text{Fe}}/\text{net acidity}$, $r^2<0.001$). Once again, this analysis is dependent on the Fe and acid species being in contact with one another in each size fraction of the aerosol. Our negative result could therefore be an indication of a low degree of internal mixing in the aerosol samples we collected, rather than that acids do not influence Fe solubility. We are not able to distinguish between these two possible causes from our dataset. However, these results appear to indicate that either enhancement of Fe solubility by acid processing of aerosol particle surfaces is not a significant process in the atmosphere per se, or that it has not occurred in the samples collected for this study because the acidic and Fe-containing aerosol fractions are not in contact with one another.

3.6. Influence of leaching protocols on solubility estimates

In this study we have estimated the solubility of several biogeochemically important aerosol components (Fe, Al, Mn, P) using simple leaching protocols. It is clear that these protocols do not realistically reproduce the conditions under which Fe, Al, Mn and P are released from aerosol particles once they are deposited onto the surface of the ocean.

In the case of our soluble metal leach, the pH chosen was too low (4.7 vs. 8.0 for seawater) and the ionic strength too high (1.1 vs. 0.73 mol L⁻¹). These factors would both be expected to enhance Fe solubility relative to seawater conditions, with the former probably the stronger effect. In addition, our experiments did not contain any strongly binding Fe chelating ligands of the type thought to be responsible for the enhancement of Fe solubility in seawater ($\log_{\text{FeL}}=13\text{--}22$; Rue and Bruland, 1995; Croot et al., 2004). Thus the relationship between our solubility estimates and ‘true’ aerosol Fe solubility will be difficult to predict, especially since Fe-binding ligand concentrations and character will vary considerably over the wide range of oceanic biogeochemical provinces that we have collected samples over. Indeed, Fe-binding ligand concentrations may even vary in response to short-term Fe inputs (Croot et al., 2001), such as may be induced by aerosol deposition. Organic ligands with the potential to bind Fe (e.g. oxalate, $\text{C}_2\text{O}_4^{2-}$) are likely to be present in ambient aerosol (e.g. Siefert et al., 1999) and such complexes would be determined in our soluble Fe leach. However, because our methods are internally consistent, we believe that the relative changes in Fe solubility observed

reflect inherent differences between aerosol types, and that these differences are most probably reflected in the ‘true’ solubility of aerosol Fe in seawater.

Soluble phosphorus leaching experiments were performed at pH 7 and an ionic strength of $\sim 1 \text{ mmol L}^{-1}$. More detailed experiments on soluble P release from an Algerian soil fraction conducted in deionised water and seawater (Ridame and Guieu, 2002) suggest that the difference between the two leachates is not great, but that our method may overestimate P solubility by up to a factor of two.

4. Conclusions

Numerous previous studies of aerosol Fe solubility (e.g. Jickells and Spokes, 2001; Bonnet and Guieu, 2004; Hand et al., 2004) have produced an extremely wide range of solubility estimates (0.001–80%), and it has been difficult to interpret this data because of the diverse methodologies used to derive those estimates. The range of aerosol Fe solubility values that we report (Table 6) is slightly lower than the range of values to be found in the published literature, but by using uniform methodology we can unambiguously ascribe this variability to differences in aerosol properties. We observe Fe solubility in Saharan dust aerosols (median 1.7%) comparable to values reported by many other workers, and consistent with the estimated overall solubility of aerosol Fe (0.8–2.1%) derived from global oceanic biogeochemical budgeting (Jickells and Spokes, 2001). In aerosols from other sources however we observe significantly higher Fe solubility (Table 6), which we attribute to some factor associated with the aerosol source (presumably aerosol chemical nature), rather than the particle concentration effect or atmospheric chemical processing of aerosol. The higher solubility of Fe in non-desert dust aerosol does not significantly affect estimates of soluble Fe input to the global ocean — desert inputs completely dominate the total input of Fe to the ocean (Duce et al., 1991; Jickells et al., 2005) and therefore also control the total input of soluble Fe to the global ocean. However, on a regional scale higher Fe solubility may be of greater importance. The ocean regions that are most sensitive to Fe inputs (the HNLC areas; Coale et al., 1996; Boyd et al., 2000) are remote from the major deserts and a higher Fe solubility for aerosol inputs to those regions may alter our understanding of Fe cycling within them. Fe (and Al) solubility in fine aerosol particles appears to be slightly higher than in coarse particles, consistent with previous studies (Siefert et al., 1999; Johansen et al., 2000; Chen and Siefert, 2004; Hand et al., 2004).

The solubility of aerosol Al is approximately a factor of 1.5 higher than Fe solubility for all aerosol types (for bulk aerosol $\text{Sol}_{\text{Al}} = 1.47 \text{ Sol}_{\text{Fe}} + 3.1$, $r^2 = 0.53$, $p < 0.01$, with similar relationships for the fine and coarse modes). This suggests that water column dissolved Al concentrations can reliably be used as a proxy for dust inputs of Fe (Measures and Vink, 2000) provided this factor is taken into account. The solubility of Mn is less variable between aerosol types, and shows no statistically significant correlations with the solubility of aerosol Fe or Al. We recently demonstrated that Atlantic aerosol is highly depleted in soluble P relative to the other nutrients (N and soluble Fe), with respect to phytoplankton requirements for these elements (Baker et al., 2003). Our measured total concentrations of aerosol P are too low to supply sufficient P relative to N to Atlantic surface waters.

Acknowledgments

We would like to thank the masters and crews of RV *Polarstern*, RRS *James Clark Ross* and RV *Pelagia*, K. Timmermanns (NOIZ) for collecting aerosol samples during IRONAGES III and K. Biswas for JCR major ions analysis. This work was supported by the EU IRONAGES programme (EVK2-1999-00031). We gratefully acknowledge the NOAA Air Resources Laboratory (ARL) for the provision of the HYSPLIT transport and dispersion model and READY website (<http://www.arl.noaa.gov/ready.html>) used in this publication. The thoughtful comments of two anonymous reviewers helped to improve the manuscript.

References

- Arimoto, R., et al., 1995. Trace elements in the atmosphere over the North Atlantic. *J. Geophys. Res.* 100, 1199–1213.
- Artaxo, P., Storms, H., Bruynseels, F., Van Grieken, R., Andreae, M.O., 1988. Composition and sources of aerosols from the Amazon Basin. *J. Geophys. Res.* 93, 1605–1615.
- Baker, A.R., 2004. Inorganic iodine speciation in tropical Atlantic aerosol. *Geophys. Res. Lett.* 31, L23S02. doi:10.1029/2004GL020144.
- Baker, A.R., Kelly, S.D., Biswas, K.F., Witt, M., Jickells, T.D., 2003. Atmospheric deposition of nutrients to the Atlantic Ocean. *Geophys. Res. Lett.* 30, 2296. doi:10.1029/2003GL018518.
- Bonnet, S., Guieu, C., 2004. Dissolution of atmospheric iron in seawater. *Geophys. Res. Lett.* 31, L03303. doi:10.1029/2003GL018423.
- Boyd, P.W., et al., 2000. A mesoscale phytoplankton bloom in the polar Southern Ocean stimulated by iron fertilization. *Nature* 407, 695–702.
- Bruland, K.W., Rue, E.L., Smith, G.J., 2001. Iron and macronutrients in California coastal upwelling regimes: implications for diatom blooms. *Limnol. Oceanogr.* 46, 1661–1674.
- Chen, Y., Siefert, R.L., 2004. Seasonal and spatial distributions and dry deposition fluxes of atmospheric total and labile iron over the

- tropical and subtropical North Atlantic Ocean. *J. Geophys. Res.* 109, D09305. doi:10.1029/2003JD003958.
- Coale, K.H., et al., 1996. A massive phytoplankton bloom induced by an ecosystem-scale iron fertilization experiment in the equatorial Pacific Ocean. *Nature* 383, 495–501.
- Croot, P.L., et al., 2001. Retention of dissolved iron and Fe-II in an iron induced Southern Ocean phytoplankton bloom. *Geophys. Res. Lett.* 28, 3425–3428.
- Croot, P.L., Andersson, K., Ozturk, M., Turner, D.R., 2004. The distribution and specification of iron along 6 degrees E in the Southern Ocean. *Deep-Sea Res., Part II* 51, 2857–2879.
- Desboeufs, K.V., Losno, R., Vimeux, F., Cholbi, S., 1999. The pH-dependent dissolution of wind-transported Saharan dust. *J. Geophys. Res.* 104, 21287–21299.
- Draxler, R.R., Rolph, G.D., 2003. HYSPLIT (HYbrid Single-Particle Lagrangian Integrated Trajectory) Model access via NOAA ARL READY Website (<http://www.arl.noaa.gov/ready/hysplit4.html>). NOAA Air Resources Laboratory, Silver Spring, MD.
- Duce, R.A., et al., 1991. The atmospheric input of trace species to the world ocean. *Glob. Biogeochem. Cycles* 5, 193–259.
- Gehlen, M., Heinze, C., Maier-Reimer, E., Measures, C.I., 2003. Coupled Al-Si geochemistry in an ocean general circulation model: A tool for the validation of oceanic dust deposition fields? *Glob. Biogeochem. Cycles* 17, 1028. doi:10.1029/2001GB001549.
- Graham, W.F., Duce, R.A., 1982. The atmospheric transport of phosphorus to the western North Atlantic. *Atmos. Environ.* 16, 1089–1097.
- Hand, J.L., et al., 2004. Estimates of soluble iron from observations and a global mineral aerosol model: biogeochemical implications. *J. Geophys. Res.* 109, D17205. doi:10.1029/2004JD004574.
- Herut, B., Krom, M.D., Pan, G., Mortimer, R., 1999. Atmospheric input of nitrogen and phosphorus to the Southeast Mediterranean: sources, fluxes, and possible impact. *Limnol. Oceanogr.* 44, 1683–1692.
- Jickells, T.D., 1999. The inputs of dust derived elements to the Sargasso Sea; a synthesis. *Mar. Chem.* 68, 5–14.
- Jickells, T.D., Spokes, L.J., 2001. Atmospheric iron inputs to the oceans. In: Turner, D.R., Hunter, K. (Eds.), *The Biogeochemistry of Iron in Seawater*. Wiley, Chichester.
- Jickells, T.D., et al., 2003. Isotopic evidence for a marine ammonia source. *Geophys. Res. Lett.* 30, 1374. doi:10.1029/2002GL016728.
- Jickells, T.D., et al., 2005. Global Iron Connections between desert dust, ocean biogeochemistry and climate. *Science* 308, 67–71.
- Johansen, A.M., Siefert, R.L., Hoffmann, M.R., 2000. Chemical composition of aerosols collected over the tropical North Atlantic Ocean. *J. Geophys. Res.* 105, 15277–15312.
- Kramer, J., Laan, P., Sarthou, G., Timmermans, K.R., de Baar, H.J.W., 2004. Distribution of dissolved aluminium in the high atmospheric input region of the subtropical waters of the North Atlantic Ocean. *Mar. Chem.* 88, 85–101.
- Losno, R., Bergametti, G., Carlier, P., 1992. Origins of atmospheric particulate matter over the North Sea and the Atlantic Ocean. *J. Atmos. Chem.* 15, 333–352.
- Mahowald, N. et al., in press-a. Impacts of biomass burning and land use on Amazonian atmospheric phosphorus cycling and deposition. *Glob. Biogeochem. Cycles*.
- Mahowald, N.M., et al., in press-b. The atmospheric global dust cycle and iron inputs to the ocean. *Glob. Biogeochem. Cycles*.
- Measures, C.I., Brown, E.T., 1996. Estimating dust input to the Atlantic Ocean using surface water Al concentrations. In: Guerzoni, S., Chester, R. (Eds.), *The Impact of Desert Dust Across the Mediterranean*. Kluwer, Dordrecht, pp. 301–311.
- Measures, C.I., Vink, S., 2000. On the use of dissolved aluminum in surface waters to estimate dust deposition to the ocean. *Glob. Biogeochem. Cycles* 14, 317–327.
- Mills, M.M., Ridame, C., Davey, M., La Roche, J., Geider, R.J., 2004. Iron and phosphorus co-limit nitrogen fixation in the eastern tropical North Atlantic. *Nature* 429, 292–294.
- Orians, K.J., Bruland, K., 1985. Dissolved aluminium in the central Pacific Ocean. *Nature* 316, 427–429.
- Paerl, H.W., 1997. Coastal eutrophication and harmful algal blooms: importance of atmospheric deposition and groundwater as “new” nitrogen and other nutrient sources. *Limnol. Oceanogr.* 42, 1154–1165.
- Parsons, T.R., Maita, Y., Lalli, C.M., 1984. *A Manual of Chemical and Biological Methods for Seawater Analysis*. Pergamon, Oxford.
- Rädlein, N., Heumann, K.G., 1992. Trace analysis of heavy metals in aerosols over the Atlantic Ocean from Antarctica to Europe. *Int. J. Environ. Anal. Chem.* 48, 127–150.
- Rädlein, N., Heumann, K.G., 1995. Size fractionated impactor sampling of aerosol particles over the Atlantic Ocean from Europe to Antarctica as a methodology for source identification of Cd, Pb, Tl, Ni, Cr, and Fe. *Fresenius’ J. Anal. Chem.* 352, 748–755.
- Raes, F., et al., 2000. Formation and cycling of aerosols in the global troposphere. *Atmos. Environ.* 34, 4215–4240.
- Ridame, C., Guieu, C., 2002. Saharan input of phosphate to the oligotrophic water of the open western Mediterranean Sea. *Limnol. Oceanogr.* 47, 856–869.
- Rue, E.L., Bruland, K.W., 1995. Complexation of iron(III) by natural organic ligands in the central North Pacific as determined by a new competitive ligand equilibration adsorptive cathodic stripping voltammetric method. *Mar. Chem.* 50, 117–138.
- Sarthou, G., et al., 2003. Atmospheric iron deposition and sea-surface dissolved iron concentrations in the East Atlantic. *Deep-Sea Res., Part I* 50, 1339–1352.
- Schulz, M., Balkanski, Y.J., Guelle, W., Dulac, F., 1998. Role of aerosol size distribution and source location in a three-dimensional simulation of a Saharan dust episode tested against satellite-derived optical thickness. *J. Geophys. Res.* 103, 10579–10592.
- Siefert, R.L., Johansen, A.M., Hoffmann, M.R., 1999. Chemical characterization of ambient aerosol collected during the southwest monsoon and intermonsoon seasons over the Arabian Sea: Labile-Fe(II) and other trace metals. *J. Geophys. Res.* 104, 3511–3526.
- Spokes, L.J., Jickells, T.D., 1996. Factors controlling the solubility of aerosol trace metals in the atmosphere and on mixing into seawater. *Aquat. Geochem.* 1, 355–374.
- Spokes, L.J., Jickells, T.D., Lim, B., 1994. Solubilisation of aerosol trace metals by cloud processing: a laboratory study. *Geochim. Cosmochim. Acta* 58, 3281–3287.
- Taylor, S.R., McLennan, S.M., 1985. *The Continental Crust: Its Composition and Evolution*. Blackwell, Oxford. 312 pp.
- Völkering, J., Heumann, K.G., 1990. Heavy metals in the near surface aerosol over the Atlantic Ocean from 60-degrees South to 54-degrees North. *J. Geophys. Res.* 95, 20623–20632.
- Zhuang, G., Yi, Z., Duce, R.A., Brown, P.R., 1992. Chemistry of iron in marine aerosols. *Glob. Biogeochem. Cycles* 6, 161–173.